GCB Bioenergy

Global Change Biology Bioenergy
BIOPRODUCTS FOR A SUSTAINABLE BIOECONOMY

RESEARCH ARTICLE OPEN ACCESS

Short Rotation Forestry Expansion Drives Carbon Sequestration in Biomass but Not in Soil

Getachew Gemtesa Tiruneh[1] | Asmamaw Alemu[2] | Jennie Barron[1] | Fantaw Yimer[3] | Erik Karltun[1]

[1]Swedish University of Agricultural Sciences, Uppsala, Sweden | [2]College of Agriculture and Environmental Sciences, University of Gondar, Gondar, Ethiopia | [3]Wondo Genet Collage of Forestry and Natural Resources, Hawassa University, Wondo Genet, Ethiopia

Correspondence: Getachew Gemtesa Tiruneh (getachew.tiruneh@slu.se)

Received: 21 March 2025 | **Revised:** 28 May 2025 | **Accepted:** 29 May 2025

Funding: The study was funded by grant 2018-05893 from the Swedish Research Council under its sustainability and resilience call, with additional funding from the Swedish University of Agricultural Sciences (SLU).

Keywords: *Acacia mearnsii* | afforestation | charcoal | fuelwood | land use change | landscape | SOC | sustainable

ABSTRACT

A significant land use change from cropland to short rotation forestry (SRF) has taken place in the northwestern (NW) Ethiopian highlands where a fast-growing tree species, *Acacia mearnsii*, is cultivated to produce charcoal for urban markets. We investigated the extent of this land use change, its impact on the landscape carbon (C) budget, and its implications for climate change mitigation by combining field studies with remote sensing. We analyzed land use and land cover changes between 2005 and 2022 using Google Earth Pro imagery and validated the result with ground truthing through field observations. We estimated C stocks using soil and biomass samples collected from *A. mearnsii* plantation fields managed by smallholder farmers across three rotations and stand ages, as well as from cropland and other major land use types. Between 2005 and 2022, 60% of the cropland in the studied district was converted to *A. mearnsii* plantations. Our analysis showed that *A. mearnsii* cultivation had the highest spatial cover in 2017. However, a disease outbreak in 2020 resulted in a 40% reduction in cultivated area by 2022 compared to 2017 levels. The expansion of *A. mearnsii* cultivation increased total landscape C stocks by 21%, equivalent to a net sequestration of 0.3 Mt CO_2 year^{-1} in the study district. This corresponded to 2.3% of Ethiopia's total annual fossil fuel emissions in 2021. The observed gain was due to C accumulation in standing biomass. In contrast, soil C stock showed a declining trend with successive rotations, though this change was not statistically significant. The main contribution of *A. mearnsii* based SRF in NW Ethiopia to the C budget is its potential to reduce dependence on natural forest for charcoal and firewood production.

1 | Introduction

Unsustainable use of fuelwood and charcoal is a major driver of forest degradation and loss, and contributes to climate change (Wassie 2020). An estimated 27%–34% of pantropical fuelwood extraction is unsustainable, with East Africa one of the hotspots (Bailis et al. 2015). In Ethiopia, more than 90% of households rely on fuelwood and charcoal for cooking (Sime et al. 2020; Yalew 2022). While much of the fuelwood is sourced close to the homesteads of the users (Dresen et al. 2014), both fuelwood and, particularly, charcoal are traded in domestic markets. The demand is substantial, and Ethiopia ranks as the second largest charcoal producer globally, following Brazil, with a production of 5.1 million tons of charcoal in 2023 (FAOSTAT 2023). A study by Alem et al. (2010) estimated that Addis Ababa alone receives 69,000 metric tons of charcoal annually.

Historical accounts suggest that forests once covered approximately 40% of the country and up to 90% of the highlands (EFAP 1994; Young et al. 2020). By 1950, natural forest cover had declined to 16% (Thomas and Bekele 2003), and further decreased to less than 4% by the 1980s (Hurni 1988). One of the major drivers for this deforestation is the illegal production of charcoal (Teketay 2001). In recent years, the trend of forest cover loss has been reversed in some parts of Ethiopia, particularly due to plantation of eucalypts on cropland or grazing land in short rotation forestry (SRF) (Alemneh et al. 2019).

The use of fast growing SRF species has the potential to contribute to renewable energy production and climate change mitigation (Djomo et al. 2013). These production systems can be regarded as close to carbon (C) neutral if negative trends in wood biomass and soil organic carbon (SOC) can be avoided. A review by Don et al. (2012) showed that SRF established on former arable land in the European Union (EU) sequestered 0.44–0.66 Mg soil C ha^{-1} y^{-1}. However, other studies have reported mixed results regarding SOC changes. Walter et al. (2015) found no significant SOC changes, while Sabbatini et al. (2016) observed a decrease in SOC following the conversion of cropland to SRF for biomass energy production. This pattern of C accumulation in biomass with limited impact on SOC is also observed in tropical regions (Lewis et al. 2019). In the Democratic Republic of Congo, SOC initially increased after land use change to *Acacia auriculiformis* A. Cunn. ex Benth. plantations but remained unchanged over successive rotations (Dubiez et al. 2019). SRF, in general, has been shown to reduce pressure on natural forests for fuelwood and contribute to mitigate greenhouse gas emissions (Makundi 2001).

A rapid land use change from traditional crop production to SRF has taken place in the Awi zone of northwest (NW) Ethiopian highlands. This change is driven by the market demand for charcoal in urban areas (Wondie and Mekuria 2018; Nigussie et al. 2020). The species cultivated is a wattle tree native to Australia. While previous studies reported the species as green wattle (*Acacia decurrens* Willd.) (Wondie and Mekuria 2018; Chanie and Abewa 2021), a recent study has reclassified it as black wattle (*Acacia mearnsii* De Wild.) (Agena et al. 2023). *A. mearnsii* is a fast-growing, evergreen leguminous tree that can grow up to a height of 11 m in 5–6 years in the Ethiopian highlands (Mekonnen et al. 2006). Its fast growth and adaptability to various environmental conditions (Midgley and Turnbull 2003) make it a suitable source of biomass for charcoal production.

The conversion of croplands to *A. mearnsii* based SRF has significantly changed the land cover in the NW part of the Ethiopian highland over the past two decades. Several studies conducted using satellite imagery analysis have reported considerable increases in vegetation cover. Wondie and Mekuria (2018) reported a 25% increase in forest cover from 1995 to 2015, while Worku et al. (2021) observed a 16% increase between 2000 and 2017. Watershed-based studies reported even higher increases, with Belayneh et al. (2020) reporting a 256% increase between 2003 and 2017 and Berihun et al. (2019) reporting a 400% increase between 2012 and 2017.

The rapid land use change from cropland to SRF alters the C dynamics of the landscape. Biomass accumulation contributes to C sequestration, with roots turnover and litterfall eventually contributing to soil C stocks. However, these gains may be offset by greenhouse gases (GHGs) emissions from charcoal production and microbial decomposition of organic matter (OM). Therefore, the overall climate impact of land use change is determined by the net C balance between sequestration and GHG emissions.

Previous studies on the *A. mearnsii* afforestation in the Awi zone of NW Ethiopia have shown considerable variation in the extent of land use change and often focused solely on afforestation rates without distinguishing between natural forest and *A. mearnsii* plantation. Furthermore, they have not separately estimated the C pools of soil and biomass. To assess the climate impact of the charcoal produced from these plantations, we need a quantitative estimate of the C stock dynamics in the landscape. Therefore, in this study, we aimed (1) to quantify the extent of land use change since the introduction of *A. mearnsii* based SRF and (2) to estimate the C sequestration in biomass and soil in a landscape perspective. Fast-growing woody trees, such as *A. mearnsii*, sequester more C in biomass than annual herbaceous crops like teff (*Eragrostis tef* (Zucc.) Trotter) (Poorter et al. 2012). Furthermore, reduced soil disturbance and increased litterfall and root turnover in tree cultivation systems contribute to increased soil C stocks (Rowe et al. 2016; Georgiadis et al. 2017). Consequently, we hypothesized that *A. mearnsii* would significantly increase both soil and biomass C stocks compared to the annual, rain-fed, *E. tef* cultivation practiced in the area.

2 | Methods

2.1 | Study Area

The study was conducted in the NW highlands of Ethiopia, in the Fagita Lekoma district (Figure 1). The district is located between 10°57′–11°11′ N and 36°40′–37°05′ E and is characterized by an undulating, sometimes steep, topography with elevations ranging from 1800 to 2900 m a.s.l (Worku et al. 2021). The main rainy season (*meher*) lasts from May to October. The annual average rainfall and temperature of the area is 2110 mm and 18°C, respectively, for the period between 1997 and 2019 (NMA 2020). The annual average temperature and rainfall data are provided in Figure S1. The soils are predominantly Acrisols, characterized by a low pH (Regassa et al. 2023).

Historically, land use in the area has been dominated by the common food crop teff (*E. tef*) cultivation, followed by barley (*Hordeum vulgare* L.), wheat (*Triticum aestivum* L.), and potato (*Solanum tuberosum* L.) (Nigussie et al. 2017). However, since the introduction of *A. mearnsii*, farmers have adopted an agroforestry system with the intercropping of *A mearnsii* and annual crops. During the initial year of seedling establishment, *A. mearnsii* is interplanted with teff. The second year the farmers harvest grass for fodder from the plantation. From the third year on, the *A. mearnsii* stands have reached a crown cover that prevents intercropping due to shading of the ground. After 5–6 years, the trees are harvested for charcoal production (Nigussie et al. 2017; Wondie and Mekuria 2018), after which a new rotation of intercropping with annual crops resumes.

2.2 | Study Approach

A space for time substitution method was used to simulate temporal dynamics associated with the land use change. The fields

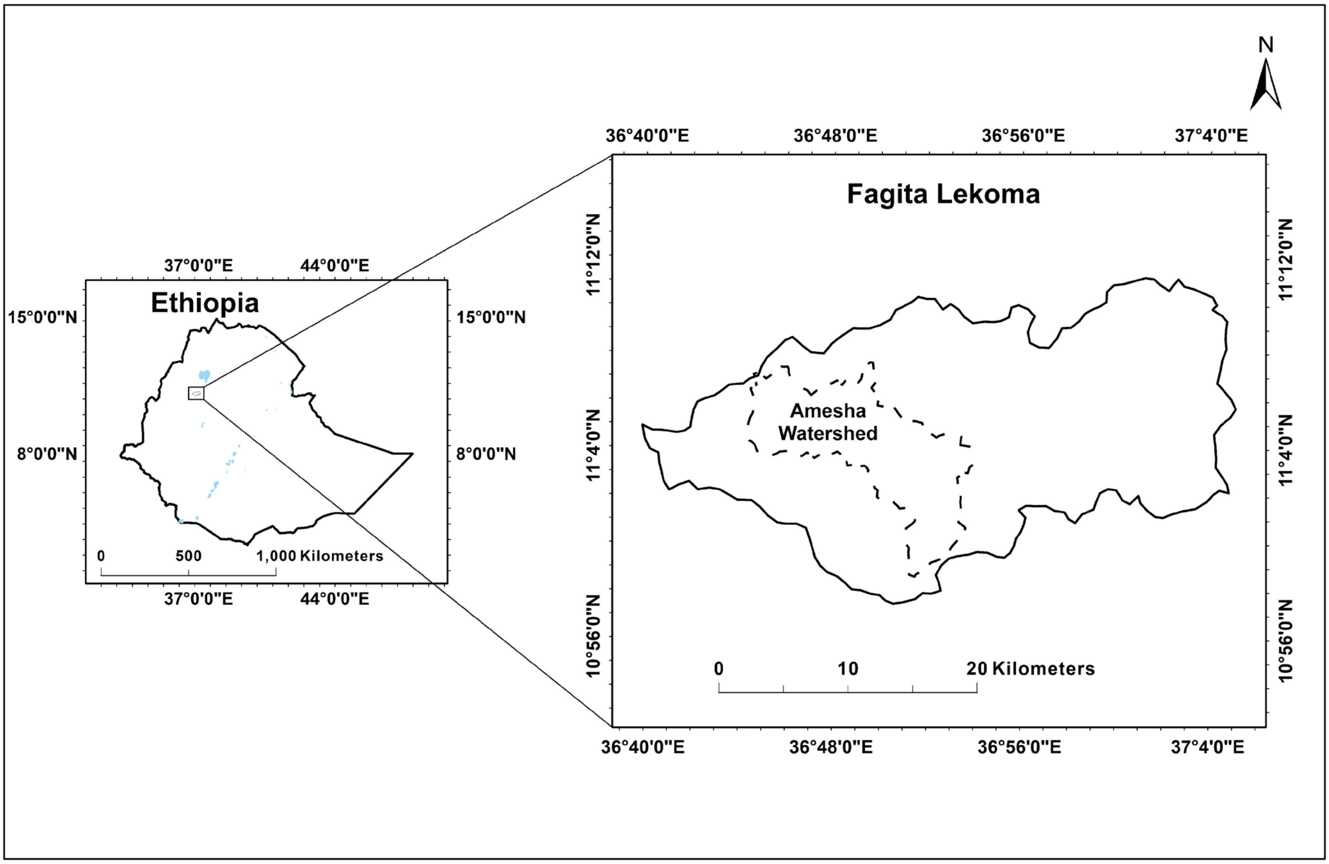

FIGURE 1 | A map of study area, Fagita Lekoma district, with the Amesha watershed delineated by dotted lines.

selected represented a chrono-sequence from cropland through successive rotations of *A. mearnsii* plantations, with stand ages ranging from three to sixyears. This approach aimed to evaluate the cumulative effects of continuous *A. mearnsii* cultivation over time. *E. tef* cultivation on cropland was the predominant land use prior to the introduction of *A. mearnsii* and represented the baseline condition. These were compared with *A. mearnsii* fields under the first, second, and third successive rotations. Additionally, fields formerly under *A. mearnsii* cultivation that had been converted back to *E.tef* cultivation (FAM), as well as natural forest and open/grazing land, were included. The FAM fields provided insights into the potential future condition of fields currently under *A. mearnsii* plantations, should cultivation be discontinued.

2.3 | Sampling Design

Soil and biomass samples were collected within the Amesha watershed in Fagita Lekoma district in April and May 2022. The watershed was delineated prior to fieldwork using the Shuttle Radar Topography Mission's (SRTM) digital elevation model from www.usgs.gov (USGS 2022) with the Hydrology tool in ArcGIS 10.7.1. This approach was adopted to fulfill the requirements of a simultaneous study within the same research project. The area of the watershed is 119 km^2.

Sampling fields were selected using a systematic random sampling technique. The delineated watershed was divided into six subareas to ensure even distribution of soil and biomass sampling. A coordinate in the center of each subarea was marked as a starting point for field selection. The resulting watershed map was subsequently uploaded to GPS devices for fieldwork navigation. Sampling teams started fieldwork by navigating to the marked center of each subarea. Upon arrival, a transect was established, and the first encountered field representing one of the predefined land use categories was selected for sampling.

Soil samples were collected from a total of 96 fields representing 16 land use categories (Figure 2). They included 72 *A. mearnsii* fields, stratified by first, second, and third rotations, and stand ages three to six. Sampling fields corresponding to each stand age and rotation were gathered from the six subareas. Fields representing the third rotation were only found near the epicenter of the early establishment of *A. mearnsii* plantations. As a result, their distribution is geographically aggregated as they were unavailable in the other subareas of the watershed. Additional samples were collected from cropland, open/grazing land, natural forest, and fields from former *A. mearnsii* plantations that have been converted back to cropland (FAM). The number of sampled fields per land use type and their corresponding definitions are provided in the Table S1.

2.4 | Soil Sampling and Analysis

In the sampling fields, a 10 m × 10 m square plot was established, and soil samples were collected from the four corners and the center of the plot at two depth intervals: 0–15 and 15–30 cm. Soil samples from the same depth at the five spots were pooled to a composite sample for each depth. Additional soil cores were collected for bulk density determination at the same depths.

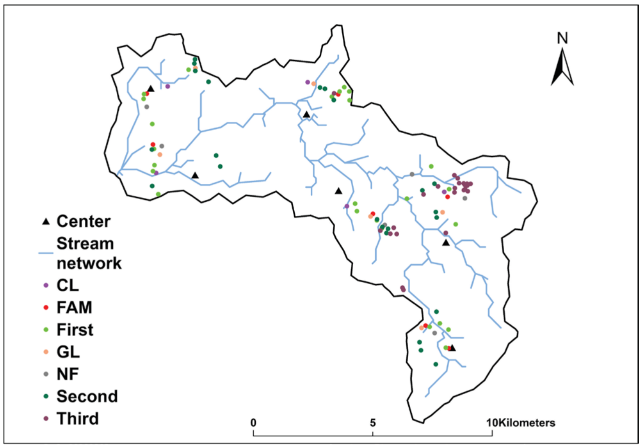

FIGURE 2 | Map of Amesha watershed with drainage networks and soil sampling locations. CL, cropland; FAM, former *Acacia mearnsii* field converted to cropland; GL, grazing land; NF, natural forest; and first, second, and third, first, second, and third rotation *A. mearnsii* plantations. Center indicates the center of each subarea marked as a starting point for field selection.

The sampled soils were air dried and crushed with a mortar and subsequently sieved through a 2 mm mesh sieve. The coarse fraction retained on the 2 mm sieve was used to calculate the coarse fraction percentage. An additional 1 g of soil was milled into fine powder using a ball mill for stable isotope analysis.

The C and nitrogen (N) content in the soils were determined through dry combustion according to ISO 10694 (1995) and ISO 13878 (1998), respectively, using an elemental analyzer (TruMac CN, Leco Corp, St. Joseph, MI, USA), with a combustion temperature of 1350°C. Soil bulk density was determined by oven drying samples at 105°C for 24 h. The bulk density was calculated by dividing the dry weight by the volume of the core sampler.

Stable isotope ratios for ^{13}C:^{12}C were determined using an isotope ratio mass spectrometer coupled with an elemental analyzer (EA-IRMS) at the stable isotope laboratory of Swedish University of Agricultural Sciences (SLU) in Umeå, Sweden. The value of the stable C isotope ratio ($^{13}C/^{12}C$) was expressed using the standard delta (δ) notation ($\delta^{13}C$) in parts per thousand (‰) relative to the Vienna Pee Dee Belemnite (VPDB) standard;

$$\delta^{13}\mathrm{C}_{(‰)} = \left(\frac{R_{\text{sample}}}{R_{\text{standard}}} - 1\right)1000 \tag{1}$$

where R is the ratio of $^{13}C/^{12}C$ in the sample and standard.

The natural abundance of $\delta^{13}C$ was used to quantify the proportion of soil C derived from *A. meanrsii*, a C3 plant introduced following land use change, and *E. tef*, a C4 crop cultivated prior to the land use change. The proportional contribution of each source to the soil C pool was calculated using the equations by Balesdent and Mariotti (1996):

$$\mathrm{C}_{\text{New}} = \left(\frac{\delta^{13}\mathrm{C}_N - \delta^{13}\mathrm{C}_\mathrm{O}}{\delta^{13}\mathrm{C}_{\mathrm{AM}} - \delta^{13}\mathrm{C}_\mathrm{O}}\right)100 \tag{2}$$

$$\mathrm{C}_{\text{New}} = \left(\frac{\delta^{13}\mathrm{C}_\mathrm{N} - \delta^{13}\mathrm{C}_\mathrm{O}}{\delta^{13}\mathrm{C}_{\mathrm{AM}} - \delta^{13}\mathrm{C}_\mathrm{T}}\right)100 \tag{3}$$

where C_{New} = proportion of C derived from *A. mearnsii* plantation in %, $\delta^{13}C_N$ = isotopic ratio of the soil under *A. mearnsii* cultivation, $\delta^{13}C_O$ = isotopic ratio of the soil under *E. tef* crop cultivation, $\delta^{13}C_{AM}$ = isotopic ratio of *A. mearnsii* biomass, and $\delta^{13}C_T$ = isotopic ratio of *E. tef* crop.

The $\delta^{13}C$ value of the *E. tef* crop (−12‰) was obtained from Krampien (2015), while the $\delta^{13}C$ values for *A. mearnsii* biomass and the soil samples were determined through laboratory analysis. Equation (3) corrects for isotopic fractions due to decomposition (Balesdent and Mariotti 1996). We report results from both equations to provide a range of potential estimates of soil C derived from *A. mearnsii*.

The soil C stock was calculated as:

$$\mathrm{CS}_i = \frac{\mathrm{SOC}_i \rho_i Z_i \left(1 - \mathrm{CF}_i\right)}{1000} 10 \tag{4}$$

where CS_i = C stock in Mg ha^{-1}, SOC_i = soil organic C (g kg^{-1}), ρ_i = soil bulk density (kg m^{-3}), Z_i = layer thickness (m), CF_i = coarse fraction > 2 mm at layer i.

Prior to C stock estimation calculation, the bulk density of the soil was adjusted according to the method specified by Fowler et al. (2023). The stock in the 0–30 cm soil depth interval was determined by summing the stock in the 0–15 and 15–30 cm layers.

2.5 | Biomass Sampling and Processing

Biomass samples were collected from *A. mearnsii* stands aged three to six in each subarea of the watershed. Plantations younger than 3 years were not present due to the impact of *Uromycladium acacia* since the beginning of 2020 (Agena et al. 2023), which led farmers to discontinue planting new trees.

In each sampling field, a 10 m × 10 m square sampling plot was established. The total number of trees within the sampling plot was recorded. Stem diameter at breast height (DBH) and tree height were measured on 20 representative trees within the sampling plot. The DBH was measured at 1.3 m above the ground using digital caliper, and tree height was measured using a graded bamboo stick. A representative tree, corresponding to the average DBH and height within the plot, was selected from each plot and destructively sampled. The tree components were separated into stem, branch, leaf, and root fractions, and subsamples were collected from each component for further analysis in laboratory. Stem samples (wood and bark) were obtained from disks cut at 20% intervals along the height of the stem. Representative samples of various sizes were taken from roots, branches, and leaves. Litter samples were collected from a set of two 30 cm × 30 cm squares placed along the diagonal of the main 10 m × 10 m square plot. Below ground biomass (BGB) was determined by excavating sample trees to 40 cm depth, with separate samples taken from

0–20 cm and 20–40 cm depths. Collected roots were classified into three diameter classes: fine (< 2 mm), medium (2–5 mm), and coarse (> 5 mm) (FAO 1990).

Fresh weights of each component were measured on site, and the corresponding dry weights were determined after oven drying a weighed subsample at 65°C until a constant weight was achieved. The C content of the litter and biomass components (stem, branches, fine and coarse roots, and leaves) was analyzed using an elemental analyzer (TruMac CN, LECO). The estimated C stocks were then converted into CO_2 equivalents to calculate CO_2 sequestration in both biomass and soil.

2.6 | Allometric Model Fitting for Estimating Biomass

Several models were tested to predict aboveground biomass (AGB) using DBH and height as predictor variables. The performance of each model was evaluated using the coefficient of determination (R^2), the root mean square error (RMSE), and the Akaike information criterion (AIC). Models with the highest R^2 and the lowest RMSE and AIC values were selected as suitable allometric equations. The goodness of fit was assessed by plotting the predicted AGB values against the observed values. The best correlation, with an R^2 value of 0.89, was obtained with the following linear model:

$$\mathrm{Ln(AGB)} = a + b\mathrm{DBH} + cH \tag{5}$$

where AGB = aboveground biomass (kg), DBH = diameter at breast height (cm), H = tree height (m), and a, b, and c are model parameters equal to 0.34, 0.026, and 0.22, respectively.

The BGB is estimated from the AGB using the following linear model:

$$\mathrm{BGB} = a + b\mathrm{AGB} \tag{6}$$

where BGB = belowground biomass (kg), AGB = aboveground biomass (kg), and a and b are model parameters equal to 0.14 and 0.076, respectively.

Biomass data for stands younger than 3 years were estimated using models built from measured data for stands aged 3–6 years and existing literature. Plant density for this age group was estimated from initial planting density and seedling counts per hectare reported by Chanie and Abewa (2021). Aboveground biomass for 1 year old stands was reported by Mekonnen et al. (2006). Aboveground biomass for 2 year old stands was estimated using a model based on data by Mekonnen et al. (2006) for stand age one and our measured data for stands aged 3–6 years. The root biomass of these stand ages was estimated as a function of above ground biomass. Litter layer C for stands aged one and two were estimated by interpolating between litter data for stands aged 3–6 years and assuming zero initial litter at planting. Similarly, soil C stocks for these stands were estimated using a similar interpolation, assuming that the average soil C stock at planting (stand aged zero) was equal to that of cropland, as most land use change was from cropland to *A. mearnsii* plantations. The resulting models and their respective R^2 values are presented in the Table S2.

2.7 | Land Cover Classification

The temporal dynamics of land use land cover (LULC) change were analyzed over a 17-year period from 2005 to 2022 using Google Earth Pro imagery (version 7.3.6.9345; accessed March 2023). Prior to classification, a 1500 m × 1500 m grid was overlaid on the Fagita Lekoma district using ArcGIS, resulting in 302 grid intersection points for LULC assessment (Figure 3a). Land use was classified at four distinct time points: 2005 when *A. mearnsii* plantations began to emerge in the area, 2014, 2017, and 2022 (Figure 3). Due to incomplete coverage in 2005, imagery from 2002 was used to fill gaps and ensure comprehensive land use classification. Imagery from the

FIGURE 3 | (a) Grid points generated in ArcGIS for land use change assessment in Fagita Lekoma. Each point was assessed at four different times: 2005, 2014, 2017, and 2022, and the type of land use and stand development at these years was recorded. The percentage of each land use type for each year was calculated as the number of points under the land use type divided by the total number of points assessed (302). (b) Grid point 519 shows the land was under cropland cultivation in 2005. (c) By 2014, this same point had been converted to *Acacia mearnsii* cultivation. (d) The previous plantation was harvested, and the site was replanted with new seedlings in 2017. (e) By 2020, the replanted *A. mearnsii* had reached a stand age of 3 years.

corresponding years was validated with ground truth data collected during fieldwork. These ground truth data were used as reference training data for visual land use classification based on Google Earth Pro imagery. The percentage of each land use type for the years studied was calculated by dividing the number of points classified under a specific land use type in a given year by the total number of points assessed (302).

TABLE 1 | Land use land cover classification studied and their respective definitions.

LULC classification	Definition
Cropland	Fields used to produce annual crops including fallow areas
Open/grazing land	Field that is used for grazing, including open areas covered with grass that may or may not have been grazed
Natural forest	Natural vegetation areas, consisting of bushes, shrubs. and woodland, developed without human interference
Acacia mearnsii plantations	Fields covered by stands of different ages and rotation cycles of *A. mearnsii* cultivation
Water bodies	Rivers and wetlands
Settlement area	Built up areas and roads
Tree lines	Defined as linear array of woody vegetation used to form a field boundary within agricultural land or alongside roads
Bare land	A barren area with exposed bedrock, gully formations, and significant erosion caused by wind or water
FAM	Fields that were formerly planted *A. mearnsii* but have since been converted back to cropland or left fallow

Subsequently, the total area for each land use type in each year was calculated by multiplying the corresponding percentage by the total area of the district. The LULC categories and their corresponding definitions are presented in Table 1.

2.8 | Statistical Analysis

The effect of land use changes on soil C stock was assessed using a mixed effect model in R using the *nlme* package (Pinheiro et al. 2025). Analyses of variance (ANOVA) were applied to examine the main effects of land use (stand age and rotation cycles for *A. mearnsii*), with site and soil depth included as a random effects. When model assumptions were not met, data were logarithmically transformed. Post hoc comparisons were performed using the *emmeans* package in R (Lenth et al. 2025) with Tukey's adjustment for multiple comparisons. Results are presented as means ± confidence intervals. The confidence interval for aggregated means represents the cumulative uncertainty propagated from individual components. Statistical significance was evaluated at $p = 0.05$.

3 | Results

3.1 | Land Use and Land Cover Change Between 2005 and 2022

Land use and land cover change between 2005 and 2022 is presented in Table 2. In 2005, cropland was the dominant land use, covering 67% of the district area, followed by open/grazing land at 19%. Other land uses collectively accounted for 14%. By 2014, both cropland and open/grazing land had decreased, while *A. mearnsii* plantations increased from 0.3% to 13% of the total area. Between 2005 and 2014, 16% of cropland and 9% of open/grazing land were converted to *A. mearnsii* plantations.

In the period between 2014 and 2017, *A. mearnsii* plantation continued to expand, primarily at the expense of croplands. By 2017, *A. mearnsii* plantations covered 42% of the total area, while cropland decreased to 29%. The conversion represented 55% of

TABLE 2 | Land use and land cover in the in Fagita Lekoma in 2005, 2014, 2017, and 2022 by area (ha) and percentage.

	2005		2014		2017		2022	
LULC	Area	%	Area	%	Area	%	Area	%
Cropland	45,351	67	37,978	56	19,436	29	17,202	25
Acacia mearnsii	223	0	8712	13	28,372	42	20,776	31
Open/grazing land	12,510	19	11,170	17	9159	14	7372	11
Natural forest	4691	7	4468	7	4245	6	4245	6
Water bodies	894	1	894	1	894	1	894	1
Settlement area	1117	2	1564	2	2010	3	2234	3
Bare land	894	1	894	1	894	1	1117	2
FAM					670	1	12,063	18
Tree lines	1787	3	1787	3	1787	3	1564	2

former cropland and 23% of former open/grazing land since the 2005 baseline (Table 3). Other land use categories experienced moderate changes during the period.

The period between 2017 and 2022 saw a slowdown in land use change to *A. mearnsii* plantations. Only 5% of cropland from prior periods was converted to new plantations (Table 4). Furthermore, this period marked a reversal in land use change, with areas previously under *A. mearnsii* cultivation reverted to cropland or left fallow. By 2022, 40% of the land under *A. mearnsii* plantations in 2017 had reversed back to crop production or was left as fallow (Table 4).

Between 2005 and 2022, the expansion of *A. mearnsii* plantations resulted in the conversion of over 28,000 ha of cropland to *A. mearnsii* plantation, representing 40% of the total area of the district (Tables 3 and 4). An additional 5000 ha of open/grazing land were also converted to *A. mearnsii* plantation. The area covered by *A. mearnsii* reached its maximum in 2017 and subsequently decreased. Despite the reduction in both cropland and open/grazing land, no natural forest areas were converted to *A. mearnsii* cultivation throughout the study period.

3.2 | Carbon Sequestration in Litter and Standing Biomass

The total C stock in *A. mearnsii* biomass and litter layer increased from $20.8 \pm 8.35\,\mathrm{Mg\,ha^{-1}}$ for stands aged three to $98.3 \pm 15.2\,\mathrm{Mg\,ha^{-1}}$ for stands aged six (Table 5). AGB accounted for the largest portion, with BGB accounting for 8.5% of the total dry matter for stands aged three to six. The average C stock in

TABLE 3 | Land use change matrix for land use class in 2005 and 2017 in the Fagita Lekoma district.

	2017									
2005	**CL**	**OGL**	**NF**	**AM**	**WB**	**ST**	**BL**	**FAM**	**TL**	**Total (2005)**
Cropland	19,212			25,021		447		670		45,350
Open/grazing land	223	9159		2904		223				12,510
Natural forest	0		4244	223		223				4691
Acacia mearnsii				223						223
Water bodies					894					894
Settlement						1117				1117
Bare land							894			894
FAM										—
Tree lines									1787	1787
Total (2017)	19,436	9159	4244	28,371	894	2011	894	670	1787	67,466

Note: Values are area in ha.
Abbreviations: AM, *A. mearnsii*; BL, bare land; CL, cropland; NF, natural forest; OGL, open/grazing land; ST, settlement; TL, tree line; WB, waterbodies.

TABLE 4 | Land use change matrix for land use class in 2017 and 2022 in the Fagita Lekoma district.

	2022									
2017	**CL**	**OGL**	**NF**	**AM**	**WB**	**ST**	**BL**	**FAM**	**TL**	**Total**
Cropland	17,176			2034		226				19,436
Open/grazing land		7372		1564			223			9159
Natural forest			4244							4244
Acacia mearnsii				16,978				11,393		28,371
Water bodies					894					894
Settlement						2011				2011
Bare land							894			894
FAM								670		670
Tree lines				223					1564	1787
Total	17,176	7372	4244	20,799	894	2237	1117	12,063	1564	67,466

Note: Values are area in ha.
Abbreviations: AM, *A. mearnsii*; BL, bare land; CL, cropland; NF, natural forest; OGL, open/grazing land; ST, settlement; TL, tree line; WB, waterbodies.

TABLE 5 | Total C stock in standing biomass and litter layer by stand age in Mg ha^{-1}.

Stand age	AGB	BGB	Total biomass	C stock in biomass	C in Litter layer	Total C in biomass and litter
3	35.1 ± 14.6	4.40 ± 1.90	39.5 ± 16.5	19.8 ± 8.24	1.01 ± 0.57	20.8 ± 8.35
4	62.9 ± 24.5	6.20 ± 2.20	69.0 ± 26.7	34.5 ± 13.4	2.05 ± 0.51	36.6 ± 13.7
5	104 ± 30.7	9.40 ± 2.70	113 ± 33.5	56.7 ± 16.7	2.64 ± 0.97	59.4 ± 16.4
6	175 ± 26.2	15.1 ± 3.30	190 ± 29.2	94.9 ± 14.6	3.36 ± 1.35	98.3 ± 15.2
Mean	94.2 ± 49.5	8.80 ± 5.20	103 ± 54.4	51.5 ± 27.2	2.26 ± 1.83	53.7 ± 13.6

Note: Values indicate mean ± CI.
Abbreviations: AGB, above ground biomass; BGB, below ground biomass.

TABLE 6 | Estimated C in BGB of *Acacia mearnsii* by size class and soil depth at the typical harvest age in Mg ha^{-1}.

Stand age	Depth	Fine root biomass	Coarse root biomass	Fine root C	Coarse root C
5	0–20	3.11 ± 0.90	3.60 ± 1.04	1.56 ± 0.45	1.80 ± 0.52
	20–40	1.34 ± 0.39	1.34 ± 0.39	0.67 ± 0.19	0.67 ± 0.19
6	0–20	4.53 ± 0.98	5.56 ± 1.20	2.27 ± 0.49	2.78 ± 0.60
	20–40	2.57 ± 0.56	2.43 ± 0.53	1.28 ± 0.28	1.21 ± 0.26
Mean	0–20	3.82 ± 1.33	4.58 ± 1.59	1.91 ± 0.67	2.29 ± 0.80
	20–40	1.95 ± 0.68	1.88 ± 0.65	0.98 ± 0.34	0.94 ± 0.33

Note: Values indicate mean ± 95% CI. roots (< 5 mm diameter) and coarse roots (> 5 mm diameter).

biomass and litter layer is 53.7 ± 13.6 Mg ha^{-1}. The litter layer represented 4.2% of the average C stock. At a typical harvest age of 5–6 years, fine roots constituted 47% of the BGB, with an estimated C stock of 2.89 Mg C ha^{-1} (Table 6). The litter layer, at the same harvest age, has an estimated C stock of 3.00 Mg C ha^{-1} (Table 5). Therefore, the total C potentially retained in the field from leaf litter and fine roots is estimated to be 1.07 Mg C ha^{-1} y^{-1}.

3.3 | Soil C Stock

The mean soil C stock of different LULC classes at two soil depths is presented in Figure 4. When combining the soil C stock for the two depths, the highest soil C stock was observed in soil under natural forest with 181 ± 54.7 Mg C ha^{-1} followed by open/grazing land and FAM with 142 ± 34.4 and 132 ± 42.7 Mg C ha^{-1}, respectively. The C stock in the reference land use, cropland, was 90.8 ± 51.1 Mg C ha^{-1}. The C stock in *A. mearnsii* cultivated soils decreased with subsequent rotation cycles but increased with stand age within each rotation (Figure 5). The average C stocks were 116 ± 28.0, 90.8 ± 18.3, and 81.3 ± 13.1 Mg ha^{-1} in the first, second, and third rotations, respectively.

Statistical analysis revealed significant differences in soil C stock among the land uses studied. Post hoc comparisons showed that the soil under natural forest had a significantly higher soil C stock compared to all other land uses, whereas the third *A. mearnsii* rotation exhibited the lowest soil C stock among all land uses. Comparison between cropland soil and soil under the three *A. mearnsii* rotations also revealed that the third *A. mearnsii* rotation had significantly lower C stock compared to the first. However, no significant differences were found between cropland and any of the *A. mearnsii* rotations.

The average C stock in the 0–30 cm of the first rotation plantation was 25.2 ± 58.2 Mg ha^{-1} higher than that of cropland. Subsequent rotations showed a lower level in C stock relative to the first rotation. The second had 25.2 ± 33.5 Mg C ha^{-1} lower and the third rotation had a further 9.50 ± 22.5 Mg C ha^{-1} lower stock (Figure 5). Consequently, the overall change in soil C stock from cropland to the third rotation cycle represents a net change of—9.46 Mg C ha^{-1}. The C change was more pronounced in the 15–30 cm layer as compared to the topsoil. The stock change at the anticipated harvest age of the first and third rotation cycles, stand ages five and six, showed a decline of 37.7 Mg ha^{-1} from the first to the third rotation, that is, over 11 years. This corresponds to an average 3.43 Mg C ha^{-1} year^{-1} decrease between the first and the third rotations.

Soil $\delta^{13}C$ values did not differ significantly between cropland and *A. mearnsii* rotation cycles ($p = 0.31$) (Table 7). The analysis showed the amount of C possibly derived from *A. mearnsii* biomass decreased with successive rotations. The estimated annual C derived from *A. mearnsii* using Equation (2) was 1.99, 1.02, and 0.58 Mg C ha^{-1} year^{-1} for the first, second, and third rotations, respectively, with an average of 1.20 Mg C ha^{-1} year^{-1} (Table 7). The estimates based on Equation (3) were 1.16, 0.59, and 0.34 Mg C ha^{-1} year^{-1} for the respective rotations, with an average of 0.70 Mg C ha^{-1} y^{-1}.

3.4 | Landscape C Balance

When total biomass and soil C under SRF are summed, and C stocks for cropland, open/grazing land and natural forest are assumed to remain constant, the total C stock in the Fagita Lekoma district increased from 6.77 ± 2.37 Tg in 2005 to

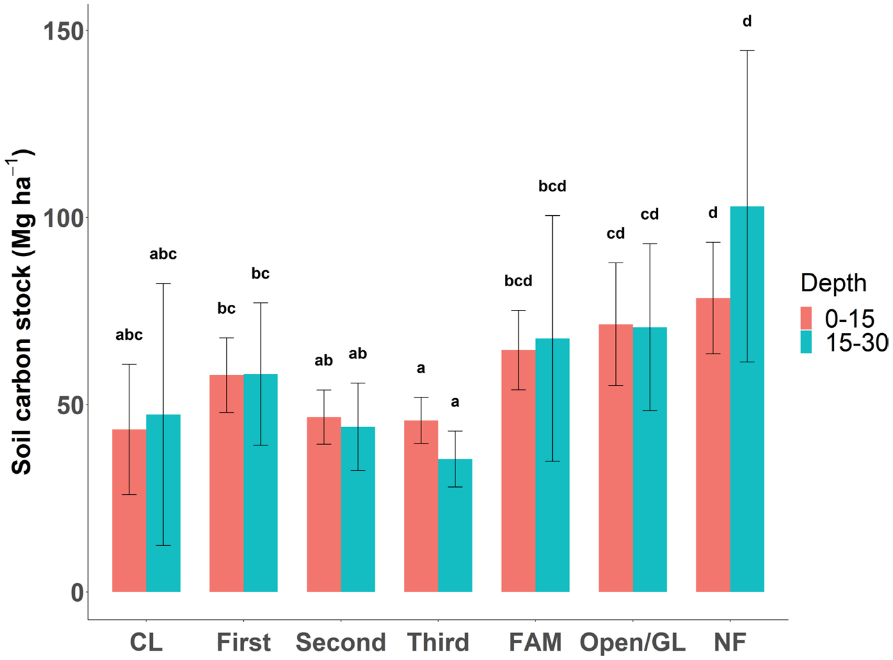

FIGURE 4 | Soil C stock at 0–15 and 15–30 cm depths across different LULC classes. First, second, and third represent the respective rotation cycles of *Acacia mearnsii*. CL, Open/GL, and NF refers to cropland, open/grazing land and natural forest, respectively. Values are mean C stock for the respective depth interval and LULC class and error bars indicate 95% confidence intervals. *A. mearnsii* rotation values are average C stock for stands aged 3–6 years. Means denoted by a different letter indicate significant differences between the land uses. The mean and CI are presented based on the orgianl data, whereas the analysis was perfomred on a logarithmic scale. Sample sizes: Cropland (5), first rotation AM (24), second rotation AM (24), third rotation AM (24), FAM (7), Open/grazing land (6), and Natural forest (6).

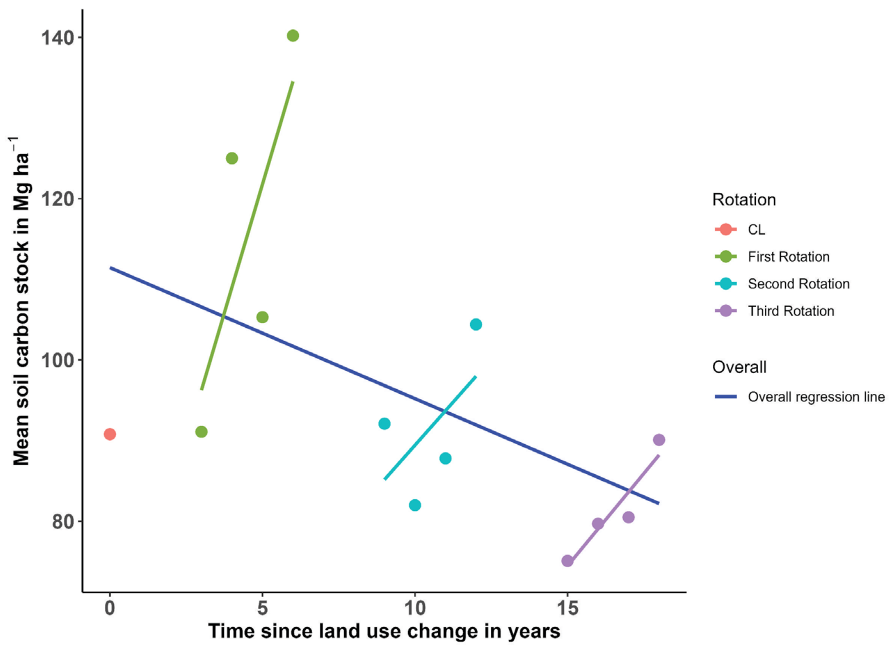

FIGURE 5 | Average soil C stock (Mg ha^{-1}) as a function of time since land use changed from cropland to *Acacia mearnsii* plantations. The organge colored point represents the average C stock of the cropland (CL) soil, serving as the initial reference soil C stock. Green points indicate the mean C stock of the first-rotation plantations with stand ages ranging from 3 to 6 years. Similarly, light blue and purple points represent the second and third rotations, respectively, with stand ages from 3 to 6 years. Regression lines for each rotation correspond to the colors of respective rotations. The blue line represents the overall regression line fitted across all stand ages since the land use conversion to *A. mearnsii* plantations. Sample sizes: Presented in Table S1; for first, second, and third rotations *A. mearnsii* plantations, each point represents a stand age of 3–6 years. Values were calculated as the average of samples per stand.

8.18 ± 1.59 Tg in 2022 with a net increase of 1.41 Tg (Figures 6 and 7). This corresponds to an overall increase of 21% between 2005 and 2022. The increase correlates with the areal expansion of *A. mearnsii* plantation, which increased from less than 1% of the area in 2005 to 42% of the area in 2017. At the same time, Google Earth Pro imagery revealed that the

TABLE 7 | δ^{13}C‰ values of soil under cropland and different rotation of *Acacia mearnsii* cultivation and corresponding estimates of C derived from *A. mearnsii*.

Land use	Depth	δ^{13}C ‰	C stock Mg ha^{-1}	% C derived from AM (Equation 2)	C derived from AM Mg ha^{-1} (Equation 2)	C derived from AM Mg ha^{-1} year^{-1} (Equation 2)	% C derived from AM (Equation 3)	C derived from AM Mg ha^{-1} (Equation 3)	C derived from AM Mg ha^{-1} year^{-1} (Equation 3)
CL	0–15	−18.6 ± 1.1	43.4 ± 17.4						
	15–30	−18.1 ± 1.3	47.4 ± 35.0						
FAM	0–15	−19.1 ± 1	64.6 ± 10.6	5.9%	3.84 ± 0.63		3.4%	2.2 ± 0.36	
	15–30	−17.8 ± 1.4	67.7 ± 32.8						
First rotation	0–15	−19.5 ± 0.8	57.9 ± 10.0	10.7%	6.19 ± 1.07	1.12 ± 0.19	6.1%	3.53 ± 0.61	0.64 ± 0.11
	15–30	−18.8 ± 0.8	58.2 ± 19.0	8.1%	4.74 ± 1.55	0.86 ± 0.28	5.0%	2.91 ± 0.95	0.52 ± 0.17
Second rotation	0–15	−20.4 ± 1.6	46.7 ± 7.20	20.5%	9.59 ± 1.48	0.87 ± 0.13	11.8%	5.51 ± 0.86	0.50 ± 0.16
	15–30	−18.4 ± 1.5	44.1 ± 11.7	3.8%	1.67 ± 0.44	0.15 ± 0.04	2.3%	1.02 ± 0.27	0.09 ± 0.02
Third rotation	0–15	−20.2 ± 1.2	45.8 ± 6.20	18.2%	8.31 ± 1.13	0.50 ± 0.07	10.4%	4.76 ± 0.64	0.29 ± 0.04
	15–30	−18.4 ± 1.4	35.5 ± 7.50	3.5%	1.26 ± 0.27	0.08 ± 0.02	2.2%	0.78 ± 0.16	0.05 ± 0.01

Note: The annual C derived from *A. mearnsii* was calculated by dividing the total C attributed to *A. mearnsii* by 5.5, 11, and 16.5 for the first, second, and third rotations, respectively. These values correspond to the cumulative years since land use change, assuming a typical harvest age of 5–6 years and an average of 5.5 years per rotation.
Abbreviation: AM, *A. mearnsii*.

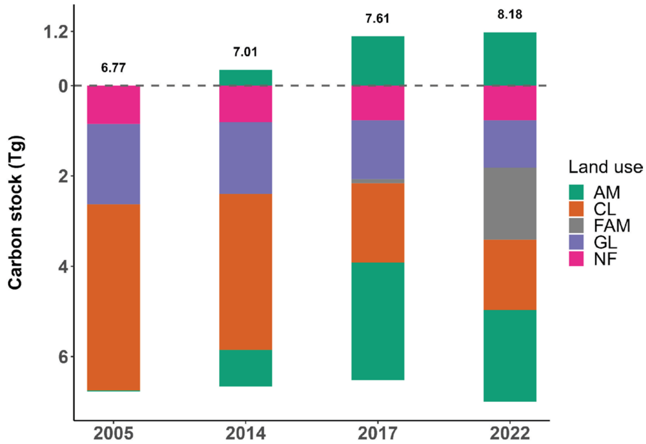

FIGURE 6 | Above- and below-ground C stocks in Fagita Lekoma from 2005 to 2022 in Tg C. The dotted zero line represents the soil surface. Bars above the dotted line indicate C stock in *Acacia mearnsii* biomass, while bars below the dotted line represent C stock in the soil. The values on the top of the bars represent the total C stock in soil and biomass for the respective years in the landscape. Note that biomass C represents only the C sequestered in *A. mearnsii* biomass. AM, land under *A. mearnsii*; CL, cropland; FAM, formerly under *A. mearnsii* plantation but reverted back to cropland; GL, open/grazing land; NF, natural forest.

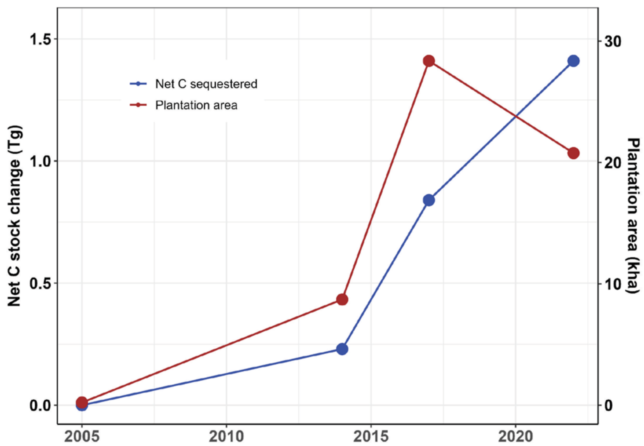

FIGURE 7 | Changes in area under *Acacia mearnsii* plantation and the corresponding net change in C stock in Fagita Lekoma between 2005 and 2022. The blue line shows the changes in net C stock in soil and biomass (left hand y-axis), and the brown line represents the area under *A. mearnsii* plantation (right hand y-axis).

forest density in areas under natural forest cover increased between 2005 and 2022 (Figure 8).

4 | Discussion

4.1 | Land Use Land Cover Change

The predominant LULC change observed during the study period was the conversion of cropland to SRF with *A. mearnsii* plantations. Based on the analysis of land use change matrix, only 38% of the initial cropland area remained cropland. Hence, 62% of the original cropland area have had at least one cycle of *A. mearnsii* plantation between 2005 and 2022. The rapid rate of conversion to plantations occurred between 2014 and 2017. This trend is likely attributable to the influence of early adopters, whose success in the prior period demonstrated the economic viability of charcoal production over food crop, thereby triggering a cascade of emulative land use decisions (Admassie and Ayele 2010). In contrast to the changes observed in cropland and open/grazing land; the natural forest areas remained unaffected throughout the study period. Although the area under natural forest did not increase, signs of recovery were observed, with forest density increasing compared to the baseline year. This suggests that *A. mearnsii* plantations are the primary source of energy for domestic consumption, potentially mitigating deforestation pressure on natural forests.

Land use change from cropland to plantation reversed between 2017 and 2022. This reversion coincided with a disease outbreak that impacted *A. mearnsii* trees, prompting farmers to revert to crop cultivation. Informal interviews conducted by the fieldwork team revealed that the emergence of the disease coincides with the onset of the COVID-19 pandemic in 2020. Due to this temporal correlation and the widespread use of the term “corona” in the media at that time, farmers colloquially referred to the disease as “corona.” A recent visit by a team of experts identified the disease as the wattle rust fungus, *U. acaciae* (Agena et al. 2023). Despite the reduction in plantation area due to the disease outbreak, *A. mearnsii* plantations remained the dominant land use in the district in 2022.

Inconsistencies in previous estimates of LULC change within the study area have posed challenges to understand the land use dynamics and quantify the associated C stock implications. The conventional land classification approaches often struggle to accurately distinguish between natural forests and plantations due to spectral overlap (Ordway 2015). The spectral similarity between natural vegetation and *A. mearnsii* plantations can confound interpretations of land cover change, potentially leading to bias in area estimation. Therefore, the accuracy of previous studies (Wondie and Mekuria 2018; Berihun et al. 2019; Belayneh et al. 2020; Worku et al. 2021) relying solely on remotely sensed data may warrant further scrutiny, particularly those employed coarser resolution imagery. Studies using Google Earth imagery have demonstrated better accuracy for land use classification in Ethiopia (See et al. 2013; Tilahun and Teferie 2015). This improved accuracy is likely due to Google Earth Pro imagery's integration of data from multiple sources, including satellite and aerial photography (Google 2024). Unlike single sensor satellite data, which often have coarser spatial resolutions, this approach provides access to high resolution mosaics (Potere 2008; Google 2024). Moreover, the use of visual interpretation in Google Earth Pro imagery allowed us to overcome the challenge of spectral overlap. It enables detailed visual interpretation of land cover features that automated methods often struggle to differentiate, thereby improving classification accuracy.

4.2 | Carbon Stock in *A. mearnsii* Biomass

There was increased biomass C accumulation with stand age in *A. mearnsii* stands, with c. 50% of the total C sequestered in the final

FIGURE 8 | Google Earth Pro satellite imagery showing temporal increase in natural forest density from 2005 to 2022. The left panels show images from 2005, while the right panels display the same areas with increased forest density in 2022.

years prior to harvest. A similar study by Mekonnen et al. (2006) showed a higher accumulation rate (77%) in the final 2 years prior to harvest (between 40 and 64 months of age). This difference may be explained by differences in soil type and disease incidence reported in our study area (Agena et al. 2023). Mekonnen et al. (2006) conducted their study under controlled conditions on more fertile Vertisols, whereas our data were collected from farmer managed fields established on nutrient poor Acrisols. These less favorable soil conditions may have contributed to the lower growth observed. Additionally, Pham et al. (2024) reported that the disease resulted in stunted growth, leading to overall low biomass production. Therefore, the lower biomass accumulation observed in our study is likely attributable to one or a combination of these limiting factors. Despite this variation, the rapid biomass accumulation observed in both studies between 5 and 6 years of age explains the practice of harvesting *A. mearnsii* for charcoal production within this age range.

The proportion of BGB in *A. mearnsii* is lower than that observed in most other tree species (Cairns et al. 1997; Qi et al. 2019). BGB have been shown to contribute more to SOC than AGB, and root derived C has a longer residence time in soils (Rasse et al. 2005). The low BGB observed in this study indicates a limited contribution to SOC through root turnover. Additionally, a significant portion of this BGB is removed during harvest as fuelwood (Chanie and Abewa 2021; Kim et al. 2022), while the AGB is harvested for charcoal production. The combination of low BGB litter input and intensive harvesting practices results in reduced organic inputs to the soil from both sources. As a result, fine roots remain the primary source of C input to the soil.

Despite biomass removal through harvest, expansion of *A. mearnsii* plantations resulted in C sequestration in the standing biomass. Between 2005 and 2022, a total of 2.63 Tg of C, equivalent to 9.64 Tg of CO_2, was sequestered in standing biomass. This accumulation was largely attributable to a large area under plantation in 2017 and the dominance of mature trees in 2022, which contained high C stocks, despite a decrease in plantation area between 2017 and 2022.

4.3 | Carbon Stock Change in Soil

Contrary to our hypothesis, the conversion of cropland to *A. mearnsii* plantation did not result in soil C accumulation. While first rotation plantations had higher soil C stock than cropland, successive rotations exhibited declining stocks, likely due to the export of the whole biomass of *A. mearnsii* for charcoal and firewood production (Nigussie et al. 2021).

The lack of statistical significance difference in $\delta^{13}C$ signatures between soil under *E. tef* cultivation and *A. mearnsii* plantations also suggests that the C3 *A. mearnsii* did not contribute a significant amount of new C to the soil previously cultivated with the C4 crop teff. However, the strength of this interpretation is limited by the lack of detailed historical land use data, and we cannot rely solely on $\delta^{13}C$ analysis. To complement this, we used data on $\delta^{15}N$ abundance that we presented in Tiruneh et al. (2025). This allowed us to quantify the N additions from the N fixing *A. mearnsii* by estimating the proportion of N derived from N_2 fixation. The soil $\delta^{15}N$ data revealed that 26% and 24% of the soil N in the second and third rotation in the 0–15 cm depth, respectively, originated from *A. mearnsii*. Through integration of this information with the soil C:N ratio, we estimated that *A. mearnsii* contributed 1.04 Mg C ha^{-1} $year^{-1}$ (Table S3), while the estimate based on $\delta^{13}C$ was 0.7–1.2 Mg C ha^{-1} y^{-1}. These estimates corresponded to the total C potentially retained in the field from leaf litter and fine roots turnover (1.07 Mg C ha^{-1} y^{-1}).

Despite this, our results showed no net C accumulation in the soil with successive rotations. Although C stock increased within each rotation as the stands aged from 3 to 6 years, subsequent rotations had lower initial C stocks compared to the average stock of the preceding rotation (Figure 5). This apparent contradiction may be attributed to the methodological challenges of excluding fine roots from soil samples (Kuzyakov et al. 2001). Although the soil samples were sieved through a 2 mm sieve prior to analysis, the possibility for some fine root biomass to remain and influence the results cannot be dismissed. Our results showed that 66% of fine roots were found in the 0–20 cm layer (Table 6), while Ceconi et al. (2008) reported an even higher proportion (86%). This high fine root density in the topsoil makes it likely that some fine root biomass was included in the soil samples, potentially resulting in an overestimation of soil C. The $\delta^{13}C$ and $\delta^{15}N$ analysis, which indicated a limited overall contribution of C but a higher proportion of *A. mearnsii* derived C in the 0–15 cm soil layer, supports the possibility of fine root inclusion. Therefore, the increase in C stocks within rotations likely reflects root biomass accumulation, whereas the decline over successive rotations indicates a genuine loss of stabilized SOC. Our argument is supported by the close correspondence between the amount of C potentially retained in the field and the estimates derived from $\delta^{13}C$ and $\delta^{15}N$ analysis. This indicates that the isotopically detected C is largely derived from root biomass rather than SOC. Thus, the soil C stocks, particularly in older stands with denser root systems, may be overestimated.

In addition to methodological factors, whole biomass harvest that results in low C input and the high litter quality of *A. mearnsii* (Xiang and Bauhus 2007), which increases the decomposition rate of legacy OM, may have played a significant role. Whole biomass harvest with repeated harvest cycles, removes essential plant nutrients, potentially leading to nutrient limitations in the soil (Dovey 2012). Studies show that nutrient limited plants secrete extracellular enzymes and organic compounds to enhance acquisition of phosphorus (P), sulfur (S), and other micronutrients (Dakora and Phillips 2002; Fujii and Hayakawa 2021). While this adaptive strategy allows plants to acquire essential nutrients, it leads to C loss through increased OM mineralization. We observed a higher BGB to AGB ratio in younger stands (Table 5), which suggests a prioritization of below ground growth during early developmental stages to enhance nutrient acquisition. This may also involve an increase in the production of root exudates and enzymes to obtain nutrients from organic sources. Our calculations demonstrated correspondence between the amount of P and S potentially mineralized from annual C mineralization (3.43 Mg C ha^{-1} y^{-1}) and the observed nutrient budget deficit for P and S in the *A. mearnsii* cultivation system (Tiruneh et al. 2025). This indicates that *A. mearnsii* cultivation may benefit from mining OM to mobilize P and S to support its growth.

Previous studies have shown that afforestation of former cropland can result in both an increase and a decrease of soil C stock, depending on the tree species and the climatic conditions of the area. Paul et al. (2002) suggested that the establishment of deciduous hardwoods or N-fixing species on cropland in tropical or subtropical regions leads to accumulation of soil C. However, litter quality from N fixing species, characterized by low C:N and C:P ratios, could potentially result in C loss (Manzoni et al. 2010; Mao et al. 2018). Studies by Chang et al. (2014) and reviews by Li et al. (2012) and Paul et al. (2002) indicate that soil C stock initially declines after afforestation of former croplands before a gradual return to the pre-afforestation level and subsequent increase. In this study, although the trend was weak ($p = 0.2$), we observed a decline in soil C stock with successive *A. mearnsii* rotations. It is possible that the soil C stock is still in a transitional phase, where steady-state and the subsequent accumulation period discussed by Li et al. (2012), Paul et al. (2002), and Chang et al. (2014) may not yet have been reached.

Soil under natural forest and open/grazing land had higher C stock exceeding both cropland and *A. mearnsii* plantations. This finding is consistent with previous research showing that undisturbed natural ecosystems have higher C stock (Poeplau and Don 2013; Assefa et al. 2017). FAM soils also had higher C stock compared to cropland and *A. mearnssii* plantation. However, given that *A. mearnsii* cultivation did not lead to an increase in soil C stock, the higher C stock observed in FAM soils cannot be attributed to the previous presence of *A. mearnsii*. This suggests that farmers may have prioritized reverting the field to cropland rather than maintaining it under *A. mearnsii* plantation, possibly because the soil has better agricultural productivity. This interpretation is supported by the observation that majority of the FAM fields had undergone only a single rotation. These fields were also not subject to SOC depletion associated with repeated harvest cycles. While the LULC change analysis showed that the natural forest area remained unaffected by SRF expansion, open/grazing land was the second most converted land use type to SRF after cropland during the study period.

Our finding differs from studies in the same area by Kim et al. (2022) and Amare et al. (2022), who reported a substantial increase in soil C stocks with *A. mearnsii* cultivation. Kim et al. (2022) observed an annual increase of 21 Mg C ha^{-1} y^{-1}, while Amare et al. (2022) reported an average increase of 40% in SOM after 4 years under plantation. Kim et al. (2022) analyzed soil samples collected from mature stands at harvest, while Amare et al. (2022) analyzed soil samples collected from stands ranging from newly planted to mature stands ready for harvest. These different sampling approaches limit the ability to analyze temporal C stock development within and across rotations. Kim et al. (2022) focused on mature stands, thereby missing C stock development with stand age, while Amare et al. (2022) missed evaluating long-term trends across successive rotations. Both studies, however, reported higher C stocks in mature stands compared to cropland. This is consistent with our result where all the mature stands in each rotation had higher C stock compared to cropland (Figure 5). However, given that they observed significant differences in mature stands but not in younger stands, we believe their results may also have been affected by the presence of fine roots in the soil samples. Furthermore, the high C sequestration rate of 21 Mg C ha^{-1} $year^{-1}$ in soil under *A.*

mearnsii cultivation reported by Kim et al. (2022) appears to be an overestimation. This value exceeds the average annual biomass C sequestered over a 6-year period in our study (16.4 Mg C ha^{-1} y^{-1}) (Table 5). Moreover, the finding by Kim et al. (2022) of a significant increase in soil C to a depth of 1 m appears unlikely, given the shallow root system of *A. mearnsii* observed in this study and corroborated by others. It is unlikely that such a substantial change in C stock to 1 m depth could appear within a three rotations period (12–16 years).

4.4 | Carbon Balance in a Landscape Perspective

Despite the observed average decrease in soil C stock with successive rotations, the large amount of C sequestered in biomass offsets the possible loss in the soil. The combined analysis of soil and biomass C stock in the Fagita Lekoma district indicated that there was an overall increase in C stock in the landscape. The increase corresponds to 5.17 Mt of CO_2 equivalent, translating to an annual CO_2 sequestration rate of 0.30 Mt. Although the district accounts for only 0.06% of the total land area of Ethiopia (UN 2024), its average annual CO_2 sink represented 2.3% of Ethiopia's total annual fossil fuel emissions for the year 2021(IEA 2022).

Our estimation of C stock changes did not account for the potential increase resulting from natural forest regeneration. The expansion of *A. mearnsii* plantations has contributed to natural forest conservation. A review of temporal imagery from Google Earth Pro showed a corresponding increase in forest density with the expansion of plantations. This suggests that the net increase in C stock in the district may be higher than estimated, considering the positive impact of the plantations on natural forest regeneration.

The main contribution of *A. mearnsii* based SRF in Fagita Lekoma to the C dynamics is its role in reducing reliance on natural forest resources for charcoal and firewood production. With biomass based energy constituting over 90% of household cooking energy source (Sime et al. 2020; Yalew 2022), the landscape's role as a C sink is expected to remain significant if cultivation continues to expand into new areas. However, long-term productivity of the production system depends on implementation of sustainable management practices (Tiruneh et al. 2025).

To the best of our knowledge, this study represents the first comprehensive landscape level analysis of C dynamics of *A. mearnsii* plantations in Ethiopia. Previous studies have primarily focused on field-scale comparisons of C stocks in cropland soils and those under *A. mearnsii* cultivation. However, while these field level studies offer valuable insights into localized C dynamics, they do not consider the spatial distribution of land use types or the temporal changes in land use patterns. Consequently, extrapolating findings from such studies to the landscape scale may result in under- or overestimations of C stock changes. We addressed this challenge by adopting a landscape level approach that integrates multiple land use types and temporal land use and land cover change over a 17-year period. This enabled us to assess not only the difference between specific land uses but also the broader impacts of land use change on C stock dynamics in the landscape.

5 | Conclusions

This study examined the impact of land use change from cropland to *A. mearnsii* based SRF on C stock dynamics. Land use and land cover change analysis showed a substantial change between 2005 and 2022, primarily from cropland to SRF. By 2017, *A. mearnsii* cultivation reached its peak, covering 42% of the area, while cropland decreased from 67% in 2005 to 25% in 2022. However, a reversal of this trend occurred after 2017, with 40% of former *A. mearnsii* planted areas reverted to cropland or left fallow, coinciding with a disease outbreak.

Conversion of cropland to *A. mearnsii* plantations did not lead to soil C accumulation. Although the initial conversion resulted in a modest increase in soil C stock, subsequent rotations showed a decline. However, these observed differences were not statistically significant, and C sequestered in biomass offsets the potential C losses in soil.

The landscape level analysis revealed an overall increase in C stock, driven by biomass C accumulation. The annual CO_2 sequestration rate of the *A. mearnsii* based SRF system in Fagita Lekoma represented 2.3% of Ethiopia's fossil fuel emission for the year 2021.

Author Contributions

Getachew Gemtesa Tiruneh: data curation, formal analysis, investigation, methodology, project administration, visualization, writing – original draft, writing – review and editing. **Asmamaw Alemu:** funding acquisition, investigation, methodology, project administration, writing – review and editing. **Jennie Barron:** funding acquisition, methodology, writing – review and editing. **Fantaw Yimer:** investigation, methodology, writing – review and editing. **Erik Karltun:** conceptualization, data curation, funding acquisition, investigation, methodology, project administration, supervision, visualization, writing – review and editing.

Acknowledgements

The study was funded by grant 2018-05893 from the Swedish Research Council under its sustainability and resilience call, with additional funding from the Swedish University of Agricultural Sciences (SLU). We wish to thank all the farmers for permission to sample their fields, and Yekoye Alene, Abebe Shume, and Adis Tedla for their assistance in soil and biomass sample collection. Tilahun Admasu, Habtamu Kifle, and Muluwork Tafa are acknowledged for their support in sample processing at the laboratory. We thank Dr. Zebene Mikru and Ethio Agri-CEFT for providing access to the company's laboratory facilities. We would also like to thank Claudia von Brömssen at SLU for her support with the statistical method used in this study.

Conflicts of Interest

The authors declare no conflicts of interest.

Data Availability Statement

Data that supports the finding of this study are openly available in Dryad at https://doi.org/10.5061/dryad.q573n5tvt.

References

Admassie, A., and G. Ayele. 2010. "Adoption of Improved Technology in Ethiopia." *Ethiopian Journal of Economics* 19: 155–179. https://doi.org/10.4314/eje.v19i1.71416.

Agena, A., K. Regasa, W. Beze, et al. 2023. "Management of *Acacia decurrens* Pests and Diseases in Ethiopia." Accessed March 3, 2024. https://www.aciar.gov.au/publication/project-final-report/fst-2021-162-final-report.

Alem, S., J. Duraisamy, E. Legesse, Y. Seboka, and E. Mitiku. 2010. "Wood Charcoal Supply to Addis Ababa City and Its Effect on the Environment." *Energy & Environment* 21: 601–609.

Alemneh, T., B. F. Zaitchik, B. Simane, and A. Ambelu. 2019. "Changing Patterns of Tree Cover in a Tropical Highland Region and Implications for Food, Energy, and Water Resources." *Frontiers in Environmental Science* 7: 1. https://doi.org/10.3389/fenvs.2019.00001.

Amare, T., T. Amede, A. Abewa, et al. 2022. "Remediation of Acid Soils and Soil Property Amelioration via *Acacia decurrens*-Based Agroforestry System." *Agroforestry Systems* 96: 329–342. https://doi.org/10.1007/s10457-021-00721-8.

Assefa, D., B. Rewald, H. Sandén, et al. 2017. "Deforestation and Land Use Strongly Effect Soil Organic Carbon and Nitrogen Stock in Northwest Ethiopia." *Catena* 153: 89–99. https://doi.org/10.1016/j.catena.2017.02.003.

Bailis, R., R. Drigo, A. Ghilardi, and O. Masera. 2015. "The Carbon Footprint of Traditional Woodfuels." *Nature Climate Change* 5: 266–272. https://doi.org/10.1038/nclimate2491.

Balesdent, J., and A. Mariotti. 1996. "Measurement of Soil Organic Matter Turnover Using 13C Natural Abundance." *Mass Spectrometry of Soils* 41, no. 3: 83–111.

Belayneh, Y., G. Ru, A. Guadie, Z. L. Teffera, and M. Tsega. 2020. "Forest Cover Change and Its Driving Forces in Fagita Lekoma District, Ethiopia." *Journal of Forestry Research* 31: 1567–1582. https://doi.org/10.1007/s11676-018-0838-8.

Berihun, M. L., A. Tsunekawa, N. Haregeweyn, et al. 2019. "Exploring Land Use/Land Cover Changes, Drivers and Their Implications in Contrasting Agro-Ecological Environments of Ethiopia." *Land Use Policy* 87: 104052. https://doi.org/10.1016/j.landusepol.2019.104052.

Cairns, M. A., S. Brown, E. H. Helmer, and G. A. Baumgardner. 1997. "Root Biomass Allocation in the World's Upland Forests." *Oecologia* 111: 1–11. https://doi.org/10.1007/s004420050201.

Ceconi, D. E., I. Poletto, T. Lovato, and M. V. Schumacher. 2008. "Biomassa e comprimento de raízes finas em povoamento de *Acacia mearnsii* De Wild estabelecido em área degradada por mineração de carvão." *Floresta* 38: 1–10. https://doi.org/10.5380/rf.v38i1.11022.

Chang, R., T. Jin, Y. Lü, G. Liu, and B. Fu. 2014. "Soil Carbon and Nitrogen Changes Following Afforestation of Marginal Cropland Across a Precipitation Gradient in Loess Plateau of China." *PLoS One* 9: e85426. https://doi.org/10.1371/journal.pone.0085426.

Chanie, Y., and A. Abewa. 2021. "Expansion of *Acacia decurrens* Plantation on the Acidic Highlands of Awi Zone, Ethiopia, and Its Socio-Economic Benefits." *Cogent Food & Agriculture* 7: 1917150. https://doi.org/10.1080/23311932.2021.1917150.

Dakora, F. D., and D. A. Phillips. 2002. "Root Exudates as Mediators of Mineral Acquisition in Low-Nutrient Environments." *Food Security in Nutrient-Stressed Environments: Exploiting Plants' Genetic Capabilities. Developments in Plant and Soil Sciences*, edited by J.J. Adu-Gyamfi, Vol. 95, 201–213. Springer. https://doi.org/10.1007/978-94-017-1570-6_23.

Djomo, S. N., O. El Kasmioui, T. De Groote, et al. 2013. "Energy and Climate Benefits of Bioelectricity From Low-Input Short Rotation Woody Crops on Agricultural Land Over a Two-Year Rotation." *Applied Energy* 111: 862–870. https://doi.org/10.1016/j.apenergy.2013.05.017.

Don, A., B. Osborne, A. Hastings, et al. 2012. "Land-Use Change to Bioenergy Production in Europe: Implications for the Greenhouse Gas Balance and Soil Carbon." *GCB Bioenergy* 4: 372–391. https://doi.org/10.1111/j.1757-1707.2011.01116.x.

Dovey, S. B. 2012. *Effects of Clear Felling and Residue Management on Nutrient Pools, Productivity and Sustainability in a Clonal Eucalypt Stand in South Africa*. Stellenbosch University. https://scholar.sun.ac.za/items/c629a0dd-d86c-4ad7-b19b-41a35482e834.

Dresen, E., B. Devries, M. Herold, L. Verchot, and R. Müller. 2014. "Fuelwood Savings and Carbon Emission Reductions by the Use of Improved Cooking Stoves in an Afromontane Forest, Ethiopia." *Land* 3: 1137–1157. https://doi.org/10.3390/land3031137.

Dubiez, E., V. Freycon, J.-N. Marien, R. Peltier, and J.-M. Harmand. 2019. "Long Term Impact of *Acacia auriculiformis* Woodlots Growing in Rotation With Cassava and Maize on the Carbon and Nutrient Contents of Savannah Sandy Soils in the Humid Tropics (Democratic Republic of Congo)." *Agroforestry Systems* 93: 1167–1178. https://doi.org/10.1007/s10457-018-0222-x.

EFAP. 1994. *Final Report Volume II—The Challenge for Development and Volume III—Issues and Action. Ministry of Natural Resources Development and Environmental Protection*. Ethiopian Forestry Action Program.

FAO. 1990. *Guidelines for Soil Description*. FAO. Accessed October 20, 2024. https://openknowledge.fao.org/handle/20.500.14283/a0541e.

FAOSTAT. 2023. *FAOSTAT Data on Forestry Production and Trade*. FAO. https://www.fao.org/faostat/en/#data/FO.

Fowler, A. F., B. Basso, N. Millar, and W. F. Brinton. 2023. "A Simple Soil Mass Correction for a More Accurate Determination of Soil Carbon Stock Changes." *Scientific Reports* 13: 2242. https://doi.org/10.1038/s41598-023-29289-2.

Fujii, K., and C. Hayakawa. 2021. "Root Exudation and Biodegradation of Organic Acids in a Tropical Forest Soil Under Dipterocarp and Pioneer Trees." *Plant and Soil* 469: 213–226. https://doi.org/10.1007/s11104-021-05132-3.

Georgiadis, P., L. Vesterdal, I. Stupak, and K. Raulund-Rasmussen. 2017. "Accumulation of Soil Organic Carbon After Cropland Conversion to Short-Rotation Willow and Poplar." *GCB Bioenergy* 9: 1390–1401. https://doi.org/10.1111/gcbb.12416.

Google. 2024. "How Images Are Collected—Google Earth Help." Google. Accessed November 22, 2024. https://support.google.com/earth/answer/6327779?hl=en&utm_source=chatgpt.com. https://support.google.com/earth/answer/6327779?hl=en&utm_source=chatgpt.com.

Hurni, H. 1988. "Degradation and Conservation of the Resources in the Ethiopian Highlands." *Mountain Research and Development* 8: 123–130. https://doi.org/10.2307/3673438.

IEA. 2022. "How Much CO_2 Does Ethiopia Emit?".

Kim, D.-G., G. Kassahun, F. Yimer, N. Brüggemann, and B. Glaser. 2022. "Agroforestry Practices and On-Site Charcoal Production Enhance Soil Fertility and Climate Change Mitigation in Northwestern Ethiopia." *Agronomy for Sustainable Development* 42: 80. https://doi.org/10.1007/s13593-022-00810-7.

Krampien, J. T. 2015. "*Faidherbia albida* Water Use and Impacts on Teff Growth in a Sub-Humid Environment in Mojo, Ethiopia." Master's Thesis, Oregon State University. https://ir.library.oregonstate.edu/concern/graduate_thesis_or_dissertations/n870zv65r.

Kuzyakov, Y., O. Biriukova, F. Turyabahika, and K. Stahr. 2001. "Electrostatic Method to Separate Roots From Soil." *Journal of Plant Nutrition and Soil Science* 164: 541–545. https://doi.org/10.1002/1522-2624(200110)164:5<541::AID-JPLN541>3.0.CO;2-H.

Lenth, R. V., B. Banfai, B. Bolker, et al. 2025. "emmeans: Estimated Marginal Means, aka Least-Squares Means." 2020. R Package Version 1.10.7. Accessed March 14, 2025. https://doi.org/10.32614/CRAN.package.emmeans. https://rvlenth.github.io/emmeans/. https://rvlenth.github.io/emmeans/.

Lewis, T., L. Verstraten, B. Hogg, et al. 2019. "Reforestation of Agricultural Land in the Tropics: The Relative Contribution of Soil, Living Biomass and Debris Pools to Carbon Sequestration." *Science of the Total Environment* 649: 1502–1513. https://doi.org/10.1016/j.scitotenv.2018.08.351.

Li, D., S. Niu, and Y. Luo. 2012. "Global Patterns of the Dynamics of Soil Carbon and Nitrogen Stocks Following Afforestation: A Meta-Analysis." *New Phytologist* 195: 172–181. https://doi.org/10.1111/j.1469-8137.2012.04150.x.

Makundi, W. R. 2001. "Potential and Cost of Carbon Sequestration in the Tanzanian Forest Sector." *Mitigation and Adaptation Strategies for Global Change* 6: 335–353. https://doi.org/10.1023/A:1013359415718.

Manzoni, S., J. A. Trofymow, R. B. Jackson, and A. Porporato. 2010. "Stoichiometric Controls on Carbon, Nitrogen, and Phosphorus Dynamics in Decomposing Litter." *Ecological Monographs* 80: 89–106. https://doi.org/10.1890/09-0179.1.

Mao, R., X. Zhang, C. Song, X. Wang, and P. M. Finnegan. 2018. "Plant Functional Group Controls Litter Decomposition Rate and Its Temperature Sensitivity: An Incubation Experiment on Litters From a Boreal Peatland in Northeast China." *Science of the Total Environment* 626: 678–683. https://doi.org/10.1016/j.scitotenv.2018.01.162.

Mekonnen, K., T. Yohannes, G. Glatzel, and Y. Amha. 2006. "Performance of Eight Tree Species in the Highland Vertisols of Central Ethiopia: Growth, Foliage Nutrient Concentration and Effect on Soil Chemical Properties." *New Forests* 32: 285–298. https://doi.org/10.1007/s11056-006-9003-x.

Midgley, S., and J. Turnbull. 2003. "Domestication and Use of Australian Acacias: Case Studies of Five Important Species." *Australian Systematic Botany* 16: 89–102. https://doi.org/10.1071/SB01038.

Nigussie, Z., A. Tsunekawa, N. Haregeweyn, et al. 2017. "Factors Affecting Small-Scale Farmers' Land Allocation and Tree Density Decisions in an *Acacia decurrens*-Based Taungya System in Fagita Lekoma District, North-Western Ethiopia." *Small-Scale Forestry* 16: 219–233. https://doi.org/10.1007/s11842-016-9352-z.

Nigussie, Z., A. Tsunekawa, N. Haregeweyn, et al. 2020. "Economic and Financial Sustainability of an *Acacia decurrens*-Based Taungya System for Farmers in the Upper Blue Nile Basin, Ethiopia." *Land Use Policy* 90: 104331. https://doi.org/10.1016/j.landusepol.2019.104331.

Nigussie, Z., A. Tsunekawa, N. Haregeweyn, et al. 2021. "Small-Scale Woodlot Growers' Interest in Participating in Bioenergy Market in Rural Ethiopia." *Environmental Management* 68: 553–565. https://doi.org/10.1007/s00267-021-01524-4.

NMA. 2020. *National Meteorological Agency*. NMA.

Ordway, E. M. 2015. "Political Shifts and Changing Forests: Effects of Armed Conflict on Forest Conservation in Rwanda." *Global Ecology and Conservation* 3: 448–460. https://doi.org/10.1016/j.gecco.2015.01.013.

Paul, K., P. Polglase, J. Nyakuengama, and P. Khanna. 2002. "Change in Soil Carbon Following Afforestation." *Forest Ecology and Management* 168: 241–257. https://doi.org/10.1016/S0378-1127(01)00740-X.

Pham, N. Q., M. J. Wingfield, S. Marincowitz, et al. 2024. "First Report of the Wattle Rust Pathogen, Uromycladium Acaciae (Raveneliaceae, Pucciniales) in Ethiopia." *Forestry: An International Journal of Forest Research* 97: 319–326. https://doi.org/10.1093/forestry/cpad040.

Pinheiro, J., D. Bates, S. Debroy, et al. 2025. "nlme: Linear and Nonlinear Mixed Effects Models." R Package Version 3.1-167. https://doi.org/10.32614/CRAN.package.nlme. https://CRAN.R-project.org/package=nlme. Accessed March 13, 2025.

Poeplau, C., and A. Don. 2013. "Sensitivity of Soil Organic Carbon Stocks and Fractions to Different Land-Use Changes Across Europe." *Geoderma* 192: 189–201. https://doi.org/10.1016/j.geoderma.2012.08.003.

Poorter, H., K. J. Niklas, P. B. Reich, J. Oleksyn, P. Poot, and L. Mommer. 2012. "Biomass Allocation to Leaves, Stems and Roots: Meta-Analyses of Interspecific Variation and Environmental Control." *New Phytologist* 193: 30–50. https://doi.org/10.1111/j.1469-8137.2011.03952.x.

Potere, D. 2008. "Horizontal Positional Accuracy of Google Earth's High-Resolution Imagery Archive." *Sensors* 8: 7973–7981. https://doi.org/10.3390/s8127973.

Qi, Y., W. Wei, C. Chen, and L. Chen. 2019. "Plant Root-Shoot Biomass Allocation Over Diverse Biomes: A Global Synthesis." *Global Ecology and Conservation* 18: e00606. https://doi.org/10.1016/j.gecco.2019.e00606.

Rasse, D. P., C. Rumpel, and M.-F. Dignac. 2005. "Is Soil Carbon Mostly Root Carbon? Mechanisms for a Specific Stabilisation." *Plant and Soil* 269: 341–356. https://doi.org/10.1007/s11104-004-0907-y.

Regassa, A., M. Assen, A. Ali, and B. Gessesse. 2023. "Major Soil Types." In *The Soils of Ethiopia*. Springer. https://doi.org/10.1007/978-3-031-17012-6.

Rowe, R. L., A. M. Keith, D. Elias, et al. 2016. "Initial Soil C and Land-Use History Determine Soil C Sequestration Under Perennial Bioenergy Crops." *GCB Bioenergy* 8: 1046–1060. https://doi.org/10.1111/gcbb.12311.

Sabbatini, S., N. Arriga, T. Bertolini, et al. 2016. "Greenhouse Gas Balance of Cropland Conversion to Bioenergy Poplar Short-Rotation Coppice." *Biogeosciences* 13: 95–113. https://doi.org/10.5194/bg-13-95-2016.

See, L., I. Mccallum, S. Fritz, et al. 2013. "Mapping Cropland in Ethiopia Using Crowdsourcing." *International Journal of Geosciences* 04: 6–13. https://doi.org/10.4236/ijg.2013.46A1002.

Sime, G., G. Tilahun, and M. Kebede. 2020. "Assessment of Biomass Energy Use Pattern and Biogas Technology Domestication Programme in Ethiopia." *African Journal of Science, Technology, Innovation and Development* 12: 747–757. https://doi.org/10.1080/20421338.2020.1732595.

Teketay, D. 2001. "Deforestation, Wood Famine, and Environmental Degradation in Ethiopia's Highland Ecosystems: Urgent Need for Action." *Northeast African Studies* 8: 53–76. http://www.jstor.org/stable/41931355.

Thomas, I., and M. Bekele. 2003. *Role of Planted Forests and Trees Outside Forests in Sustainable Forest Management in the Republic of Ethiopia*. FAO (No. FP/29E). https://www.fao.org/4/j1552e/j1552e00.htm.

Tilahun, A., and B. Teferie. 2015. "Accuracy Assessment of Land Use Land Cover Classification Using Google Earth." *American Journal of Environmental Protection* 4: 193–198. https://doi.org/10.11648/j.ajep.20150404.14.

Tiruneh, G. G., A. Alemu, J. Barron, F. Yimer, and E. Karltun. 2025. "Nutrient Budgets in Short Rotation Black Wattle (*Acacia mearnsii*) Stands for Charcoal Production as Compared With Teff (*Eragrostis tef*) Cultivation." *Forest Ecology and Management* 588: 122762. https://doi.org/10.1016/j.foreco.2025.122762.

UN. 2024. *World Population Prospects 2024*. UN Department of Economic and Social Affairs Population Devision. Accessed March 24, 2025. https://population.un.org/dataportal/data/indicators/49/locations/231/start/1990/end/2025/line/linetimeplot?df=42ff7ab7-32ed-4030-9ef9-5b39181d23eb.

USGS. 2022. "Shuttle Radar Topography Mission (SRTM) Degital Elevation Model (DEM)." Accessed on 25 March 2022. https://www.usgs.gov/.

Walter, K., A. Don, and H. Flessa. 2015. "No General Soil Carbon Sequestration Under Central European Short Rotation Coppices." *GCB Bioenergy* 7: 727–740. https://doi.org/10.1111/gcbb.12177.

Wassie, S. B. 2020. “Natural Resource Degradation Tendencies in Ethiopia: A Review.” *Environmental Systems Research* 9: 1–29. https://doi.org/10.1186/s40068-020-00194-1.

Wondie, M., and W. Mekuria. 2018. “Planting of Acacia Decurrens and Dynamics of Land Cover Change in Fagita Lekoma District in the Northwestern Highlands of Ethiopia.” *Mountain Research and Development* 38: 230–239. https://doi.org/10.1659/Mrd-Journal-D-16-00082.1.

Worku, T., M. Mekonnen, B. Yitaferu, and A. Cerdà. 2021. “Conversion of Crop Land Use to Plantation Land Use, Northwest Ethiopia.” *Trees, Forests and People* 3: 100044. https://doi.org/10.1016/j.tfp.2020.100044.

Xiang, W., and J. Bauhus. 2007. “Does the Addition of Litter From N-Fixing *Acacia mearnsii* Accelerate Leaf Decomposition of *Eucalyptus globulus*?” *Australian Journal of Botany* 55: 576–583. https://doi.org/10.1071/BT06083.

Yalew, A. W. 2022. “The Ethiopian Energy Sector and Its Implications for the SDGs and Modeling.” *Renewable and Sustainable Energy Transition* 2: 100018. https://doi.org/10.1016/j.rset.2022.100018.

Young, N. E., P. H. Evangelista, T. Mengitsu, and S. Leisz. 2020. “Twenty-Three Years of Forest Cover Change in Protected Areas Under Different Governance Strategies: A Case Study From Ethiopia's Southern Highlands.” *Land Use Policy* 91: 104426. https://doi.org/10.1016/j.landusepol.2019.104426.

Supporting Information

Additional supporting information can be found online in the Supporting Information section.